Developing a paper-based antigen assay to differentiate between coronaviruses and SARS-CoV-2 Spike variants

Delyan R. Hristov[a], Hom Rijal[b], Jose Gomez-Marquez,[c] and Kimberly Hamad-Schifferli[a, d*]

[a]Department of Engineering, University of Massachusetts Boston, Boston, MA, USA
[b]Department of Chemistry, University of Massachusetts Boston, Boston, MA, USA
[c]Little Devices Lab, Massachusetts Institute of Technology, Cambridge, MA USA
[d]School for the Environment, University of Massachusetts Boston, Boston MA, USA

ABSTRACT: COVID-19 first appeared in December of 2019 in Wuhan, China. Since then it has become a global pandemic. A robust and scalable diagnostics strategy is crucial for containing and monitoring the pandemic. RT-PCR is a known, reliable method for COVID-19 diagnostics which can differentiate between SARS-CoV-2 and other viruses. However, PCR is location dependent, time consuming and relatively expensive. Thus, there is a need for a more flexible method which may be produced in an off-the-shelf format and distributed more widely. Paper-based immunoassays can fulfill this function. Here we present the first steps towards a paper-based test which can differentiate between different between the Spike protein of various coronaviruses, SARS-CoV-1, SARS-CoV-2 and CoV-HKU1 with negligible cross reactivity for HCoV-OC43 and HCoV-229E in a single assay which takes less than 30 minutes. Furthermore, our test can distinguish between fractions of the same Spike protein. This is done by an altered assay design with four test line locations where each antigen builds a unique, identifiable binding pattern. The effect of several factors, such as running media, immunoprobe concentration and antigen interference is considered. We find that running media has a significant effect on the final binding pattern where human saliva provides results while human serum leads to the lowest signal quality.

Introduction

The COVID-19 global pandemic which emerged in Wuhan, China in December of 2019 has infected millions of people and caused or contributed to the death of hundreds of thousands and led to an economic downturn. Diagnosis of COVID-19 using diagnostic tools is preferable over clinical symptoms due to the nonspecific nature of COVID-19 symptomology. The majority of patients suffer non-specific, mild symptoms mostly consisting of cough, fever, muscle pain and nausea. [1-2] Additionally, an estimated 20 – 80% of patients are asymptomatic, with varying reports.[3-5] Traditional laboratory diagnostics such as RT-PCR have high sensitivity and diagnostic accuracy, but are expensive and time-consuming, and may not be locally available. Paper-based immunoassays can compliment PCR and contribute to a better diagnostics strategy. While they commonly suffer from relatively low selectivity and especially sensitivity, compared to PCR, paper-based tests are cheap to produce locally or in a at-scale manufacturing facility, can be made in an off-the-shelf format and stored for prolonged periods of time in mild conditions, *e.g.* room temperature or 4 °C.[6] Furthermore, ther flexible design allows simultaneous detection of multiple targets.[7-8]

Paper-based tests for SARS-CoV-2 detection can be classified as antibody (or serological) tests, *i.e.* those which measure the host immune response, and antigen tests, i.e. those which bind to viral antigens.[9] Antigen paper-based immunoassays typically target the Spike (S) or Nucleocapsid (N) proteins. The S protein decorates the outside of coronaviruses and enables their uptake into cells. [10] Variances in S protein structure determine the cellular uptake pathway and affinity of the virus for the cell. SARS-CoV-2, similarly to SARS-CoV-1 and HCoV-NL63, targets the ACE2 receptor in the oral and nasal cavities as its primary root of infection.[11-12] The S protein has been shown to be a primary driver of viral evolution, where mutations greatly impact virus infection rate and is considered to be the primary difference in reproductive number between clades.[13-14]

A low-cost, rapid, and user-friendly platform which can differentiate is desirable. Distinguishing between respiratory viruses with similar clinical symptoms is especially important not only to provide timely treatment but also better assess patient risk. Here, we present the first step towards developing a paper-based sensor which can differentiate between S proteins from different coronaviruses as well as Spike protein variants from SARS-CoV-2. The test relies on a sandwich

immunoassay and antibody cross-reactivity for antigen specific test patterns. We used a set of six commercially available antibodies and seven commercially available S proteins to establish the viability of the strategy. The test was able to differentiate between all antigens, including SARS-CoV-2 Spike fragments. Test limit of detection (LOD) was in the 0.1 nM range, which may be sufficient for viral detection in more severe cases. We also studied the effect of running medium on test efficacy, bovine serum albumin (BSA) human serum (HS) and saliva.[15]

Results

Immunoprobe Screening

We chose spike protein as a target because it protrudes outside the viral particle and is responsible for receptor recognition. It is composed of two parts, S1 and S2, where the receptor binding domain (RBD) is in S1.[16] We obtained S1 proteins for SARS-CoV-2, SARS-CoV-1 (SARS) and non-lethal coronaviruses CoV-HKU1 (HKU1), HCoV-OC43 (OC43) and HCoV-229E (229E) to study the selectivity of our nanoparticle-antibody conjugates (NP-Ab conjugates or immunoprobes). SARS-CoV-2 was termed COVID to avoid confusion (**Table 1** and **S1**).

Table 1. Antigens, antibodies and NP-Ab conjugates used

Antigens		Antibodies		
Antigen	Virus	Antibody	NP-Ab	Virus
COVID 1	SARS-CoV-2	αC1	NP-αC1	SARS-CoV-2
COVID 2	SARS-CoV-2	αC2	NP-αC2	SARS-CoV-2
COVID 3	SARS-CoV-2	αS1	NP-αS1	SARS-CoV-1
SARS	SARS-CoV-1	αS2	NP-αS2	SARS-CoV-1
229E	HCoV-229E	αS3	NP-αS3	SARS-CoV-1
OC43	HCoV-OC43	αH	NP-αH	CoV-HKU1
HKU1	CoV-HKU1			

All antibodies used were commercially available. Six antibodies were evaluated for antigen binding and sandwich immunoassay formation (**Table 1** and **S2**). Two were raised against SARS-CoV-2 (αC1-2), three for SARS (αS1-3), and one for CoV-HKU1 (αH). Gold NP-Ab conjugates were synthesized using literature methods.[17-18] Briefly, each antibody was conjugated to the NPs by physisorption, and then thiolated PEG was added after conjugation to backfill open areas on the NP surface. Dynamic light scattering (DLS) and UV-Vis spectroscopy were used to determine colloidal stability and size dispersion in PBS. DLS was used to measure particle size in BSA, saliva and HS. DLS of NPs showed hydrodynamic diameters (D_H) of ~65 nm which increased ~85 nm after antibody conjugation, supporting conjugation (**SI Figures S1, S2**). The size further increased to 120 – 200 nm in media, possibly due to protein adsorption to the NP surface.

Antibody target and off-target binding were studied using antigen and sandwich dipstick assays. In the former case the

antigens were immobilized on nitrocellulose following which the prepped strips were immersed in an immunoprobe dispersion (**Figure 1a**). In the latter case sandwich immunoassay formation, that is binding between the paper printed antibody, antigen and immunoprobe, was tested (**Figure 1c**). α-rabbit IgG Fc (α-Fc), was immobilized at the control area during both tests. A signal at the test line certified fluid flowed through the paper strip. Localized signal emerges on the strip due to immunoprobe accumulation (**Figure 1a and c**). NP-αS2 and NP- αS3 NPs were eliminated due to poor performance in initial tests (**SI Figure S3**).

After running, strips were left to dry overnight at room temperature after which they were scanned and analyzed via ImageJ.[19] The resulting grayscale values were normalized to 100% and plotted as a heatmap for clarity (**Figure 1b**), where white represents low intensity (< 20% of maximum value) and green high. Averaged grayscale values are provided in the Supporting Information.

In antigen binding tests, NP-αC1 and NP-αC2 bound to both COVID and SARS antigens, but not other coronavirus antigens. NP-αS1 bound to its target antigen, SARS, and exhibited some cross reactivity for COVID 1 and OC43. Immunoprobe binding in saliva resulted in similar signal intensities, but were notably lower in human serum (HS) (**Figure 1b, S4** and **S5**), which could be attributed to HS screening of the immunoprobe function.[9]

We evaluated the ability of the immunoprobes to form an immunological sandwich in a dipstick assay (**Figure 1c**).[20] Sandwich formation relies on two reactions, immunoprobe-antigen and printed antibody-antigen binding. The choice of both antibodies is primary during test design, where antibody pairs (on the immunoprobe / printed on the paper) with varying affinity and selectivity for a target can be used to detect a wider variety of antigens and develop a binding pattern.[21] In this initial study we screened the pairing of an antibody with itself, *i.e.,* NP-αS1 run with immobilized αS1 (NP-αS1/αS1), NP-αC1 with αC1 (NP-αC1/αC1), NP-αC2 with αC1 (NP-αC2/αC1), and NP-αH with αH (NP-αH/αH). αC2, a monoclonal antibody, did not form a sandwich with itself.

NP-αC1/αC1 and NP-αC2/αC1 were able to successfully form sandwich immunoassays with both COVID and SARS antigens, as indicated by the color resulting at the test line (**Figure 1d, S6** and **S7**). NP-αS1/αS1 was able to detect the SARS antigen, but not COVID antigens. The observed difference in behavior is potentially due to protein folding. NP-αC1/αC1 and NP-αC2/αC1 exhibited no cross reactivity for 229E, OC43, and HKU1, and NP-αH/αH exhibited signal only with HKU1.

Pairs were also tested in saliva and HS (**Figure 1d**), and the behavior was largely similar to BSA except for NP-αH/αH exhibiting some cross reactivity towards OC43 in saliva. Saliva resulted in similar intensities to BSA, but intensities were significantly lower in HS, highlighting the importance of the biological media. Generally, direct antigen binding had a higher signal and cross reactivity than sandwich formation (**Figure 1b and d**).
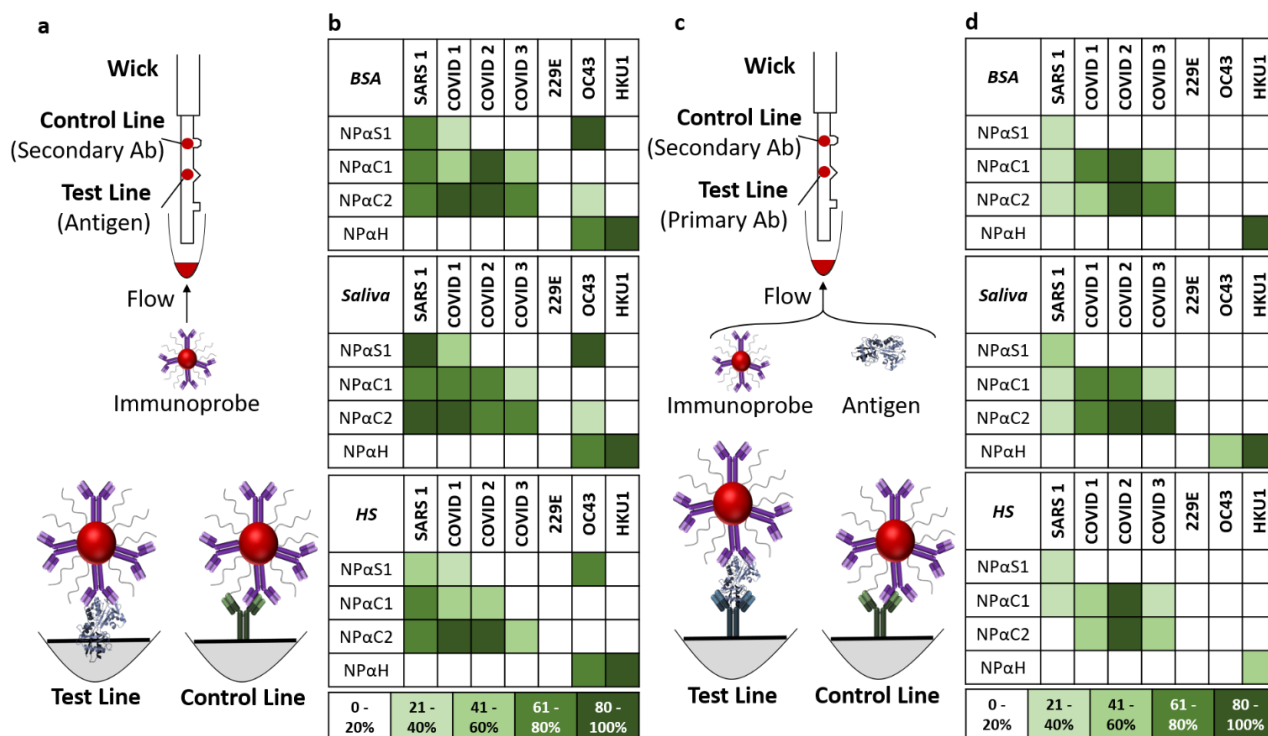
Figure 1. Antibody screening. a) Experimental setup for direct antigen binding tests and b) average test area intensities run in triplicate in BSA, saliva, and HS; c) Experimental setup for sandwich immunoassays, d) average test area intensities in BSA, saliva, and HS. Intensities were of all strips were normalized. Averaged results are from at least three independent batches. Related grayscale values and standard deviations are shown in **SI Figure S5** and **S7**.

Cross reactivity was more commonly observed in saliva compared to the other media. This could be attributed to slower flow possibly due to surface tension,[22] which results in longer residence time of the immunoprobe-antigen complex near the test areas, and increases binding probability. A compounding factor could be saliva composition, which has different surfactants or macromolecules and a lower pH (6-7)[23-24] compared to BSA and HS (7.4). We expect another large contributor to be the relatively low protein concentration of saliva, which is > 99% water (wt/wt) and ~ 1 mg/mL protein[22] compared to BSA (30 mg/mL) and HS (60 – 80 mg/mL). Test backgrounds in all three media were similar, suggesting low non-specific binding of the immunoprobes to the paper.

Antigen cross reactivity could be attributed to proximity in phylogeny. Cross reactivity between SARS and SARS-CoV-2 antibodies and antigens was expected due to ~82% sequence similarities,[13, 25-26] while the proximity between the RBD regions is ~73%.[13] NP-αH bound to its target antigen HKU1, as well as OC43 presumably due to proximity in phylogeny.[10] Antigen sequences were compared between each other and the Wuhan reference strain structure (accession number YP_009724390.1) using MUSCLE (**SI Figure S8a**). Structural differences in MUSCLE can arise from both sequence length and content therefore it is expected that some structural dissimilarities arise our antigens being recombinant fractions of the S protein. HKU1 was most dissimilar shoring the most structural similarity with the Wuhan reference strain (20%) and the least with COVID 1 (10%). SARS had a ~50% structural similarity with COVID 1 and 2 and ~28% with COVID 3 and the Wuhan reference train. Similarity between the COVID antigens and compared with the Wuhan strain were 30-50%. Comparison of the RBD of all COVID antigens revealed a 100% structural similarity (**SI Figure S8b**). COVID 1 had a 98% similarity with the Wuhan strain (**SI Figure S8c**).

Quantifying sandwich immunoassay performance in different media

Performance of the sandwich immunoassays was investigated by quantifying their limit of detection (LOD) and effective dissociation constant (K_D^{Eff}) for their target antigens. NP-αC1/αC1, NP-αC2/αC1, and NP-αH/αH, were titrated with COVID 1 and HKU1 antigens in BSA, HS and saliva. Test line intensities were measured and fit with a modified Langmuir equation.[17-18, 27] K_D^{Eff} was obtained from the fitting. LOD was calculated separately, defined as the background signal + 3x the standard deviation of the background (**SI, Calculations section**). LODs ranged from 0.1 to 0.17 nM while K_D^{Eff} values were in the 10^{-10} M range (**Figure 2a-c, Table 1 and S3**).

Changing the running media impacted performance. Compared to BSA, antibody pairs generally performed similarly or better in saliva and worse in HS (**Figure 2a-c, Table 1**). The LOD of NP-αC1/αC1 was lowest in BSA and 2X higher in saliva and 7x in HS (**Figure 2a** and **Table 1**). Titration curves of NP-αC2/αC1 were lowest in BSA, followed by saliva (3x), and significantly higher in HS (9x) (**Figure 2b**).

Between the two SARS-CoV-2 pairs, NP-αC1/αC1 exhibited comparable behavior, but marginally outperformed NP-αC2/αC1 in all media by ~2X. This is consistent with sandwich results where NP-αC1/αC1 which had a higher intensity with COVID 1 than NP-αC2/αC1. NP-αH/αH behavior changed the most with running media, where LOD and K_D^{Eff} values varied by two orders of magnitude between saliva and HS. LODs were 0.07 nM in saliva and 0.54 nM in HS. K_D^{Eff} values were 0.06 nM in saliva and 2.78 nM in HS (**Table 1, Figure 2c, d**).
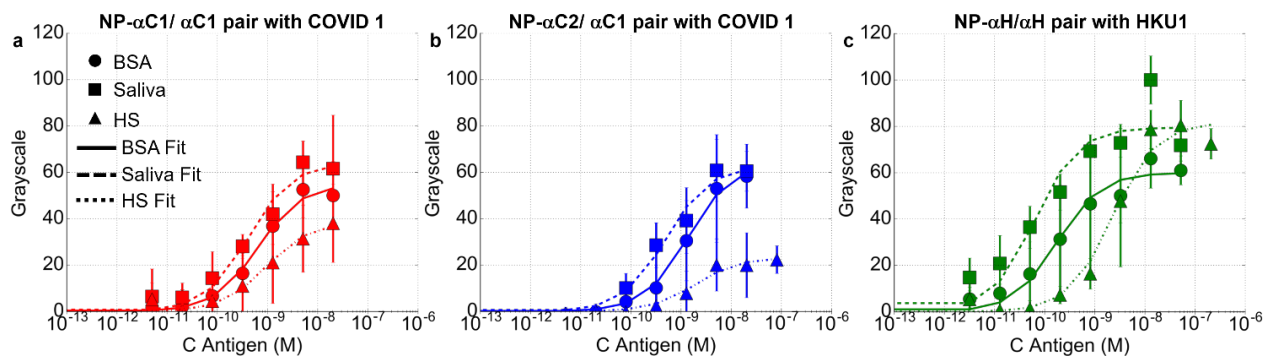
Figure 2. Immunoprobe performance. Titration curves of selected pairs. a) NP- αC1/αC1 run with COVID 1, b) NP- αC2/αC1 run with COVID 1, c) NP- αH1/αH1 run with HKU1.

Control of antigen detection through cross reactivity

We then investigated how the test could be used a multiplexed test to differentiate between SARS-CoV-2 antigens with similar structure and other coronavirus species, building on the ability to strategically use cross-reactive antibodies to differentiate between different antigens.[21] We first studied the relevance of both binding events on sandwich formation and antigen detection. The signal of combinations of all three antigens (SARS, COVID 1 and HKU1), immunoprobes (NP-αC1, NP-αC2, NP-αH) and printed antibodies (αS1, αC1, αH) was measured (total of 27 combinations, **Figure S9a**). Experiments were repeated in triplicate in BSA at antigen concentrations of 1×10^{-3} mg/mL.

SARS was detectable only with the NP-αC1/αS1 and NP-αC2/αS1 pairs. COVID 1 was detectable only with the NP-αC1/αC1 and NP-αC2/αC1 pairs, and HKU1 was detectable only with the NP-αH/αH pair (**SI Figure S9b** and **c**). This further confirmed HKU1 was not cross reactive with the other coronavirus antibodies.

These results reaffirm the efficacy of the cross reactivity strategy, where only SARS was detected at immobilized αS1 and only COVID 1 at immobilized αC1. We attribute this to the lower affinity of cross reactive interactions, which was confirmed by off target antigen titrations (**SI Figure S10**). The NP-αC1/αC1 and NP-αS1/αC1 antibody couples were titrated with their "off target" antigens, being SARS and COVID 1, respectively (**SI Figure S10 and Table S4 and S5**). Both showed reduced signal in all media compared to their "on target" immunoprobe performance. There was no significant difference in LOD and K_D^{Eff} for NP-αC1/αC1 compared to its "on-target" COVID 1 titration (**Table S4 and S5**).

Our results suggest that detection of SARS and COVID 1 is more dependent on the printed antibody rather than the one conjugated to the AuNP. On average, there was an order of magnitude drop in "off target" interactions, compared to "on target ones", e.g. NP-αC1/αS1 to NP-αC1/αC1 with SARS (**SI Figure S9b-c**). Overall these results suggest that cross reactivity can be used for generating patterns.

Multiplexed test

We designed multiplexed assay to differentiate between spike antigens of SARS, COVID 1, 2 and 3 and simultaneously detect spike from a non-lethal coronavirus, HKU1. The strip consisted of a control and four test areas at differently shaped locations (**Figure 3a**). Choice of location shape was to differentiate locations easier. Test area geometry did not have a measurable impact on signal quality. The antibodies immobilized at the test locations were (bottom to top) αS1 (square), αC2 (triangle), αC1 (octagon) and αH (oblong). A 1:1 volumetric mixture of NP-αC1 and NP-αH was used to detect all antigens.

Table 2. LOD and K_D^{Eff} values of pairs for target antigens in BSA, saliva, and HS.

	BSA		Saliva		HS	
	LOD (nM)	K_D^{Eff} (nM)	LOD (nM)	K_D^{Eff} (nM)	LOD (nM)	K_D^{Eff} (nM)
NP-αC1/ αC1 with COVID 1	0.08	0.41	0.24	0.26	0.59	0.6
NP-αC2/αC1 with COVID 1	0.17	0.88	0.56	0.32	1.56	1.28
NP-αH/αH with HKU1	0.03	0.18	0.07	0.06	0.54	2.78

Running the assay with the different antigens produced characteristic binding patterns at the four test areas. SARS and COVID antigens were detectable on all locations except the αH area (oblong) in saliva (**Figure 3b**). SARS resulted in signal mostly at the αS1 location, with lower signals at αC1 and αC2. COVID 1 exhibited the highest signal at αC2 and lower signal with αC1 and αS1 (**Figure S3b**). COVID 2 was only detectable at αC areas with comparable signal intensity at both locations (**Figure 3b**). As expected from its structure, COVID 3 produced signal mostly at the αC2 area. 229E and OC43 antigens in saliva yielded no significant signal, and HKU1 was observable only at the αH test area.
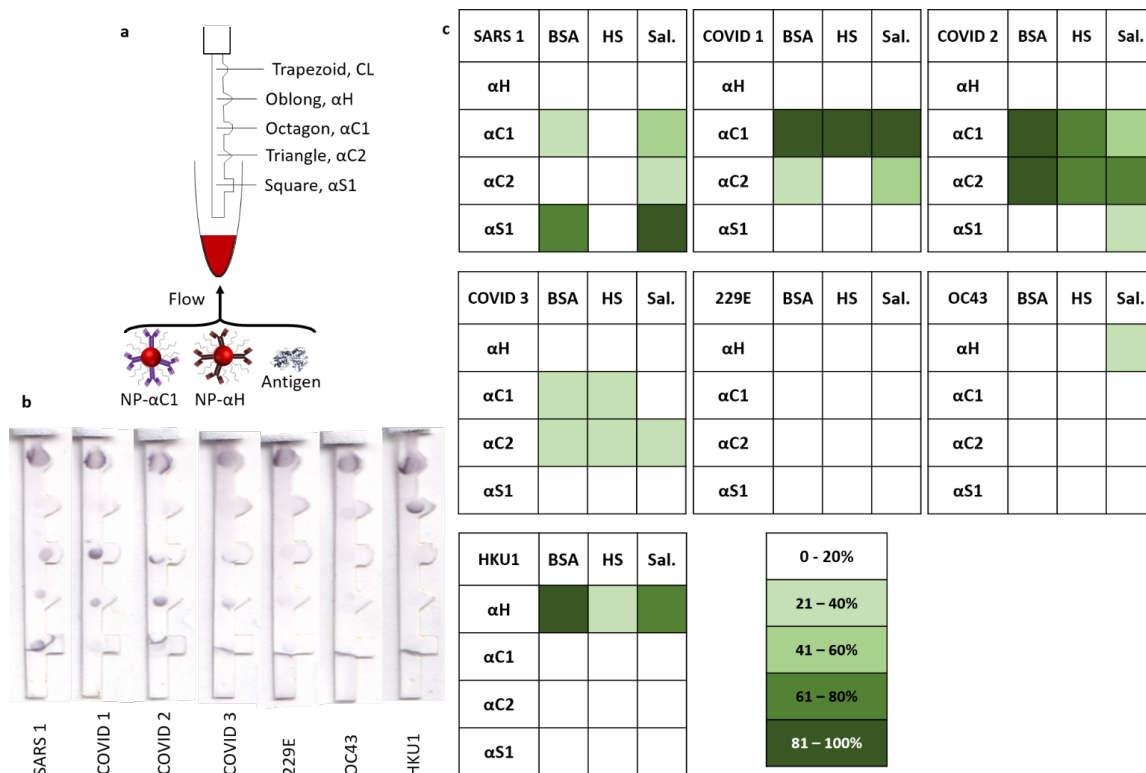
Figure 3. Altered strip design and antigen binding patterns. a) schematic of experimental procedure, b) example strips run in saliva, c) average test area intensities run in triplicate in BSA, saliva, and HS. Intensities of all strips were normalized. Grayscale values for test shown in **SI Figure S11**.

Again, signals were similar in BSA and saliva but were either reduced in intensity or lost in HS. For example, SARS could not be detected in HS, but display a characteristic pattern in BSA and saliva (**Figure 3c, top left**). HKU1 signal was strongest in BSA and weakest in HS, which was consistent with single strip results (**Figures 1d, 2c**). Cross reactivity was observed more often in saliva, where SARS was detectable at the αC2 location, COVID 2 was detectable at the αS1 location and OC43 was detectable at the αH location.

Interference between multiple antigens in multiplexed test

We ran antigen mixtures in our test to investigate binding interference (**Figure 4a**). When a mixture of SARS + HKU1 was run, intensity appeared at all four test areas, with higher intensity at αH and αS1. This pattern resembled the additive intensity pattern of SARS alone plus HKU1 alone (**Figure 4b** and **SI Figure S13e, i, j**). This suggested that the antigens did not compete with each other for forming immunoassay pairs.

Results suggest that the binding pattern in the presence of multiple antigens is similar to mathematically adding the two independent patterns if the two antigens did not bind to the same immunoprobe, e.g. SARS 1 and HKU1 (**Figure 4b**, **S13** and **S14**).

However, for antigens which bind to the same immunoprobe, the pattern depended on the affinity of the interaction. When a mixture of SARS1 + COVID 1 + HKU1 was run, intensity appeared at all four test areas, showing that the test was able to simultaneously detect SARS, COVID1 and HKU1. However, the intensity pattern did not resemble what would be anticipated from simply adding the intensities of the individually run antigens (**Figure 4c**). Since SARS and COVID 1 interact with NP-αC1 with a similar dissociation constant (K_D^{Eff}(SARS) = 0.86 nM, K_D^{Eff}(COVID 1) = 0.42 nM) the pattern of the mixture depended on the relative con-

centration of the two antigens. In this case, the antigen with the higher concentration would have a more pronounced pattern (**SI Figure S12 and S13a, b, f and S14a, b, f**). Similar effects were observed for a SARS, COVID 1 and 2 mixture (K_D^{Eff}(COVID 2) = 0.10 nM, **SI Figure S12**).

Some challenges arose with the multiplexed strip. Background gradients were more common in longer strips. To accommodate for this, we limited the strip to 5 test locations and modified the image analysis. We immobilized antibodies with higher affinity further up the strip so they would not deplete the immunoprobe/antigen complexes before they encountered lower affinity immobilized antibodies. An optimal immunoprobe or immunoprobe mixture concentration was determined to be 12-17% of the total sample volume (**SI Figure S15**).

By understanding and controlling these principles, it was possible to simultaneously detect and differentiate all three coronavirus antigens (**Figure 4c**, **SI Figure S13** and **S14**).

Discussion

The paper-based immunoassay investigated here was able to differentiate spike antigens from different coronaviruses by building a binding pattern through the number, arrangement and specificity of printed antibodies. Differentiation between SARS-CoV-1, SARS-CoV-2 and HKU1 S1 proteins was simpler based on their patterns where SARS bound mostly to the NP-αC1/αS1 pair while HKU1 bound exclusively to NP-αH/αH. Negligible cross reactivity with 229E and OC43 was observed.
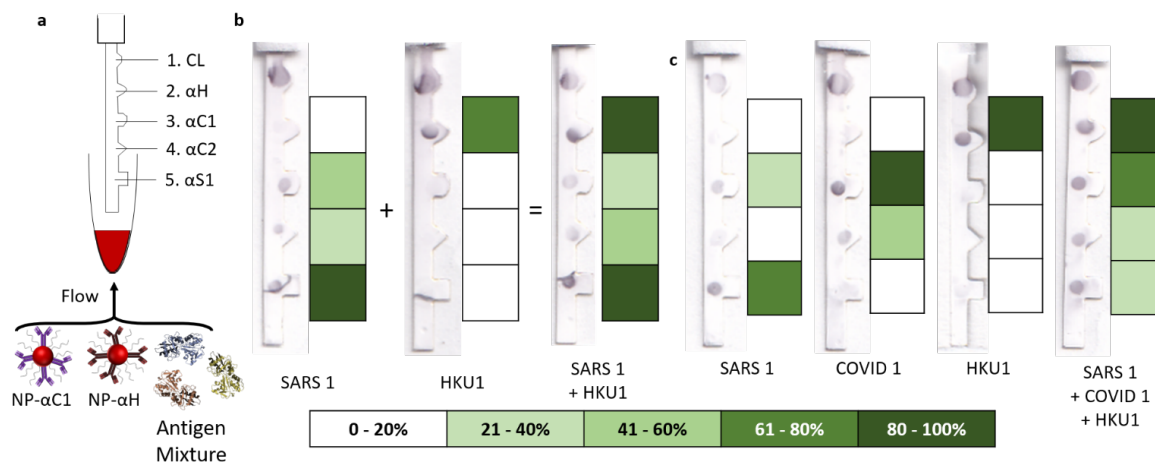
Figure 4. Running antigen mixture in altered strip design. a) Schematic of experimental procedure, b) example strips, patterns and from a test run with SARS 1 + HKU1 and c) SARS1 + COVID 1 + HKU1.

The ability to differentiate between SARS-CoV-2 antigens is especially interesting and could yield new information for patient samples. We applied our test to three recombinant S1 fragments, COVID 1 with a length of 681 amino acids (aa), COVID 2 with 461 aa and COVID 3 with 229. Considering the high similarity in sequence (**SI Figure S8**) the difference in binding pattern can be attributed to their size. Thus, the use of binding patterns may be able to differentiate between different Spike products in patient samples. This may help address some of the questions raised about patient viral shedding over time.[28] Differentiation between Spike protein variants or fractions may be improved by increasing the specificity and number of antibodies printed on the nitrocellulose. It is unlikely that the test design would be able to differentiate between Spike proteins from different clades due to high sequence similarity (> 99%).

The ability to detect and differentiate between antigen from other coronaviruses and antigen mixtures should not be overlooked. Co-circulation of non-lethal coronaviruses, other respiratory viruses and SARS-CoV-2 has been reported.[29-31] Co-infections between SARS-CoV-2 with other respiratory viruses are rare, reported in 3-20% of cases, including co-infections with non-lethal coronaviruses in about 0.1-5% of cases. [32-33] However, rare a recent study in the UK suggests that co-infection of SARS-CoV-2 with infuenza has been shown to increase risk for poor patient outcomes.[29] Co-infection may also help explain reported abnormal viral shedding patterns and differences in patient outcomes, so a test that can simultaneously differentiate between common respiratory viruses would help address these questions.

The running media impacted antigen binding, where strips run in BSA and saliva had comparable results with a 15% variation in signal, lower than test-to-test variability. Running assays in HS resulted in a reduction or complete loss of signal, which could be attributed to protein screening effects.[17, 34] LODs for COVID antigens in BSA and saliva were in the ~ng/mL range (0.03 to 0.56 nM). In comparison, others have reported similar performance with a LOD of 0.62 ng/ml (0.0125 nM) for half strips for SARS-CoV-2 nucleocapsid (N) proteins.[20, 35] We caveat that the LOD measurement was based on purified antigens in solution and not the full virus capsid in biological fluids, and matrix effects in patient samples or differences in spike secondary structure could influence performance. We estimate that the average number of Spike proteins in sputum swabs may be in the pM range for most cases and

nM range in more severe cases. This estimate is based on the average copies of RNA per mL of saliva[36] and the average number of spike proteins on a single virus.[37] We assume that every RNA copy corresponds to a virus, that each virus has 100 Spikes on its surface and there are no free Spike proteins. This is a rough estimate due to the assumptions made (**SI Calculations section**). While the concentration of spike protein in patient samples over time has still not been definitively quantified, it is anticipated that the LOD here may be too high for visual readouts for most patient samples.[37-40]

The intensity in a paper-based sandwich immunoassay depends on multiple factors, such as antibody affinity, immunoprobe concentration, antibody coverage on the NP, its size, concentration of the immobilized capture antibody, and several others.[9] Varying these parameters can improve signal intensity without external enhancement approaches. Commercial diagnostics have solved this with dedicated readers for colorimetric or fluorescent readouts (Sofia, Quidel Corp.). Surface enhanced Raman spectroscopy (SERS) nanotags,[41-42] isotachaphoresis,[43] and photothermal heating [44] have all been used successfully to increase signal, sometimes as high as 100-fold. Simply running the flow back and forth over multiple passes can increase signal 5-fold, and does not require additional readout instrumentation.[7] Additionally, concentrating the antigen by sample preparation techniques or paperfluidic design could increase signal. Ultimately, this sensitivity gap could be solved by a combination of techniques.[45]

Test variability was estimated through the standard deviation and relative standard deviation (RSD) from all tests (**SI Figure S16**), and was estimated to be 36%, which did not change significantly between media or antigen mixtures. Typically, lower signals and weaker antigen-antibody interactions resulted in higher RSDs.

Results presented here can be used towards the development of COVID-19 paper-based dipstick and lateral flow assays (LFAs), a rapid diagnostic format that has aided in disease management, quarantine, and surveillance. The low production cost and relative ease of use of paper rapid diagnostics makes them suitable for both local and large scale production, making it a potentially powerful off-the-shelf complement to RT-PCR, which could help elevate strain on local diagnostic facilities to meet the massive demand for tests. The self-contained nature of paper-based tests makes them attractive for remote or mobile locations.

ASSOCIATED CONTENT

Supporting Information contains secondary figures and tables providing context for the text, calculations used and methods section. This material is available free of charge via the Internet at http://pubs.acs.org.

AUTHOR INFORMATION

Corresponding Author

*kim.hamad@umb.edu

Author Contributions

DRH designed and carried out the studies, and wrote and edited the manuscript, HR and JGM wrote and edited the manuscript, KHS designed the studies, wrote and edited the manuscript.

ABBREVIATIONS

BSA, bovine serum albumin; DLS, dynamic light scattering; HS, human serum; LOD, limit of detection; NP, nanoparticle; RSD, relative standard deviation.

REFERENCES

1. Fu, L.; Wang, B.; Yuan, T.; Chen, X.; Ao, Y.; Fitzpatrick, T.; Li, P.; Zhou, Y.; Lin, Y.-f.; Duan, Q.; Luo, G.; Fan, S.; Lu, Y.; Feng, A.; Zhan, Y.; Liang, B.; Cai, W.; Zhang, L.; Du, X.; Li, L.; Shu, Y.; Zou, H., Clinical characteristics of coronavirus disease 2019 (COVID-19) in China: A systematic review and meta-analysis. *Journal of Infection* **2020,** *80* (6), 656-665.

2. Docherty, A. B.; Harrison, E. M.; Green, C. A.; Hardwick, H. E.; Pius, R.; Norman, L.; Holden, K. A.; Read, J. M.; Dondelinger, F.; Carson, G.; Merson, L.; Lee, J.; Plotkin, D.; Sigfrid, L.; Halpin, S.; Jackson, C.; Gamble, C.; Horby, P. W.; Nguyen-Van-Tam, J. S.; Ho, A.; Russell, C. D.; Dunning, J.; Openshaw, P. J. M.; Baillie, J. K.; Semple, M. G., Features of 20 133 UK patients in hospital with covid-19 using the ISARIC WHO Clinical Characterisation Protocol: prospective observational cohort study. *BMJ* **2020,** *369*, m1985.

3. Buitrago-Garcia, D.; Egli-Gany, D.; Counotte, M. J.; Hossmann, S.; Imeri, H.; Ipekci, A. M.; Salanti, G.; Low, N., Occurrence and transmission potential of asymptomatic and presymptomatic SARS-CoV-2 infections: A living systematic review and meta-analysis. *PLOS Medicine* **2020,** *17* (9), e1003346.

4. Ing, A. J.; Cocks, C.; Green, J. P., COVID-19: in the footsteps of Ernest Shackleton. *Thorax* **2020,** *75* (8), 693.

5. Petersen, I.; Phillips, A., Three Quarters of People with SARS-CoV-2 Infection are Asymptomatic: Analysis of English Household Survey Data. *Clinical Epidemiology* **2020,** *12* (12), 1039-1043.

6. Wang, J.; Yiu, B.; Obermeyer, J.; Filipe, C. D. M.; Brennan, J. D.; Pelton, R., Effects of Temperature and Relative Humidity on the Stability of Paper-Immobilized Antibodies. *Biomacromolecules* **2012,** *13* (2), 559-564.

7. Phillips, E.; Young, A. K.; Albarran, N.; Butler, J.; Lujan, K.; Hamad-Schifferli, K.; Gomez-Marquez, J., Ampli: A Construction Set for Paperfluidic Systems. *Advanced Healthcare Materials* **2018,** 1800104.

8. Sanchez-Purra, M.; Roig-Solvas, B.; Rodríguez-Quijada, C.; Leonardo, B.; Hamad-Schifferli, K., Design of Nanotags for Multiplexed Surface Enhanced Raman Spectroscopy Assays. *ACS Omega* **2018,** *3* (9), 10733–10742.

9. Hristov, D. R.; Rodríguez-Quijada, C.; Gomez-Marquez, J.; Hamad-Schifferli, K., Designing Paper-Based Immunoassays for Biomedical Applications. *Sensors* **2019,** *19* (3), 554.

10. Chen, B.; Tian, E.-K.; He, B.; Tian, L.; Han, R.; Wang, S.; Xiang, Q.; Zhang, S.; El Arnaout, T.; Cheng, W., Overview of lethal human coronaviruses. *Signal Transduction and Targeted Therapy* **2020,** *5* (1), 89.

11. Radzikowska, U.; Ding, M.; Tan, G.; Zhakparov, D.; Peng, Y.; Wawrzyniak, P.; Wang, M.; Li, S.; Morita, H.; Altunbulakli, C.; Reiger, M.; Neumann, A. U.; Lunjani, N.; Traidl-Hoffmann, C.; Nadeau, K. C.; O'Mahony, L.; Akdis, C.; Sokolowska, M., Distribution of ACE2, CD147, CD26, and other SARS-CoV-2 associated molecules in tissues and immune cells in health and in asthma, COPD, obesity, hypertension, and COVID-19 risk factors. *Allergy* **2020,** *75* (11), 2829-2845.

12. Rezaei, M.; Ziai, S. A.; Fakhri, S.; Pouriran, R., ACE2: Its potential role and regulation in severe acute respiratory syndrome and COVID-19. *Journal of Cellular Physiology* **2020,** *n/a* (n/a).

13. Rehman, S. U.; Shafique, L.; Ihsan, A.; Liu, Q., Evolutionary Trajectory for the Emergence of Novel Coronavirus SARS-CoV-2. *Pathogens* **2020,** *9* (3).

14. Li, Q.; Wu, J.; Nie, J.; Zhang, L.; Hao, H.; Liu, S.; Zhao, C.; Zhang, Q.; Liu, H.; Nie, L.; Qin, H.; Wang, M.; Lu, Q.; Li, X.; Sun, Q.; Liu, J.; Zhang, L.; Li, X.; Huang, W.; Wang, Y., The Impact of Mutations in SARS-CoV-2 Spike on Viral Infectivity and Antigenicity. *Cell* **2020,** *182* (5), 1284-1294.e9.

15. Azzi, L.; Maurino, V.; Baj, A.; Dani, M.; d'Aiuto, A.; Fasano, M.; Lualdi, M.; Sessa, F.; Alberio, T., Diagnostic Salivary Tests for SARS-CoV-2. *Journal of Dental Research* **2020,** 0022034520969670.

16. Walls, A. C.; Park, Y.-J.; Tortorici, M. A.; Wall, A.; McGuire, A. T.; Veesler, D., Structure, Function, and Antigenicity of the SARS-CoV-2 Spike Glycoprotein. *Cell* **2020,** *181* (2), 281-292.e6.

17. Hristov, D.; Pimentel, A. J.; Ujialele, G.; Hamad-Schifferli, K., The immunoprobe aggregation state is central to dipstick immunoassay performance. *ACS Applied Materials & Interfaces* **2020,** *12* (31), 34620-34629.

18. Tam, J. O.; de Puig, H.; Yen, C.-w.; Bosch, I.; Gómez-Márquez, J.; Clavet, C.; Hamad-Schifferli, K.; Gehrke, L., A Comparison of Nanoparticle-Antibody Conjugation Strategies in Sandwich Immunoassays. *Journal of Immunoassay and Immunochemistry* **2017,** *38* (4), 355-377.

19. Schneider, C. A.; Rasband, W. S.; Eliceiri, K. W., NIH Image to ImageJ: 25 years of image analysis. *Nature Methods* **2012,** *9* (7), 671-675.

20. Cate, D.; Hsieh, H.; Glukhova, V.; Bishop, J. D.; Hermansky, H. G.; Barrios-Lopez, B.; Grant, B. D.; Anderson, C. E.; Spencer, E.; Kuhn, S.; Gallagher, R.; Rivera, R.; Bennett, C.; Byrnes, S. A.; Connelly, J. T.; Dewan, P. K.; Boyle, D. S.; Weigl, B. H.; Nichols, K. P., Antibody Screening Results for Anti-Nucleocapsid Antibodies Towards the Development of a SARS-CoV-2 Nucleocapsid Protein Antigen Detecting Lateral Flow Assay. *ChemRxiv* **2020.**

21. Rodríguez-Quijada, C.; Gomez-Marquez, J.; Hamad-Schifferli, K., Repurposing old antibodies for new diseases by exploiting cross reactivity and multicolored nanoparticles. *ACS Nano* **2020,** *14* (6), 6626-6635.

22. Kazakov, V. N.; Udod, A. A.; Zinkovych, I. I.; Fainerman, V. B.; Miller, R., Dynamic surface tension of saliva: General relationships and application in medical diagnostics. *Colloids and Surfaces B: Biointerfaces* **2009,** *74* (2), 457-461.

23. Baliga, S.; Muglikar, S.; Kale, R., Salivary pH: A diagnostic biomarker. *Journal of Indian Society of Periodontology* **2013,** *17* (4), 461-465.

24. Humphrey, S. P.; Williamson, R. T., A review of saliva: Normal composition, flow, and function. *Journal of Prosthetic Dentistry* **2001,** *85* (2), 162-169.

25. Chen, W.-H.; Hotez, P. J.; Bottazzi, M. E., Potential for developing a SARS-CoV receptor-binding domain (RBD)

recombinant protein as a heterologous human vaccine against coronavirus infectious disease (COVID)-19. *Human Vaccines & Immunotherapeutics* **2020,** *16* (6), 1239-1242.

26.   Wu, Y., Strong evolutionary convergence of receptor-binding protein spike between COVID-19 and SARS-related coronaviruses. *bioRxiv* **2020**, 2020.03.04.975995.

27.   de Puig, H.; Bosch, I.; Carre-Camps, M.; Hamad-Schifferli, K., Effect of the protein corona on antibody-antigen binding in nanoparticle sandwich immunoassays. *Bioconjugate Chemistry* **2017,** *28* (1), 230-238.

28.   Cevik, M.; Kuppalli, K.; Kindrachuk, J.; Peiris, M., Virology, transmission, and pathogenesis of SARS-CoV-2. *BMJ* **2020,** *371*, m3862.

29.   Owusu, M.; Annan, A.; Corman, V. M.; Larbi, R.; Anti, P.; Drexler, J. F.; Agbenyega, O.; Adu-Sarkodie, Y.; Drosten, C., Human Coronaviruses Associated with Upper Respiratory Tract Infections in Three Rural Areas of Ghana. *PLOS ONE* **2014,** *9* (7), e99782.

30.   Dijkman, R.; Jebbink, M. F.; Gaunt, E.; Rossen, J. W. A.; Templeton, K. E.; Kuijpers, T. W.; van der Hoek, L., The dominance of human coronavirus OC43 and NL63 infections in infants. *Journal of Clinical Virology* **2012,** *53* (2), 135-139.

31.   Heimdal, I.; Moe, N.; Krokstad, S.; Christensen, A.; Skanke, L. H.; Nordbø, S. A.; Døllner, H., Human Coronavirus in Hospitalized Children With Respiratory Tract Infections: A 9-Year Population-Based Study From Norway. *The Journal of Infectious Diseases* **2019,** *219* (8), 1198-1206.

32.   Kim, D.; Quinn, J.; Pinsky, B.; Shah, N. H.; Brown, I., Rates of Co-infection Between SARS-CoV-2 and Other Respiratory Pathogens. *JAMA* **2020,** *323* (20), 2085-2086.

33.   Kondo, Y.; Miyazaki, S.; Yamashita, R.; Ikeda, T., Coinfection with SARS-CoV-2 and influenza A virus. *BMJ Case Reports* **2020,** *13* (7), e236812.

34.   Salvati, A.; Pitek, A. S.; Monopoli, M. P.; Prapainop, K.; Bombelli, F. B.; Hristov, D. R.; Kelly, P. M.; Åberg, C.; Mahon, E.; Dawson, K. A., Transferrin-functionalized nanoparticles lose their targeting capabilities when a biomolecule corona adsorbs on the surface. *Nature Nanotechnology* **2013,** *8* (2), 137-143.

35.   Grant, B. D.; Anderson, C. E.; Williford, J. R.; Alonzo, L. F.; Glukhova, V. A.; Boyle, D. S.; Weigl, B. H.; Nichols, K. P., SARS-CoV-2 Coronavirus Nucleocapsid Antigen-Detecting Half-Strip Lateral Flow Assay Toward the Development of Point of Care Tests Using Commercially Available Reagents. *Analytical Chemistry* **2020,** *92* (16), 11305-11309.

36.   Wölfel, R.; Corman, V. M.; Guggemos, W.; Seilmaier, M.; Zange, S.; Müller, M. A.; Niemeyer, D.; Jones, T. C.; Vollmar, P.; Rothe, C.; Hoelscher, M.; Bleicker, T.; Brünink, S.; Schneider, J.; Ehmann, R.; Zwirglmaier, K.; Drosten, C.; Wendtner, C., Virological assessment of hospitalized patients with COVID-2019. *Nature* **2020,** *581* (7809), 465-469.

37.   Bar-On, Y. M.; Flamholz, A.; Phillips, R.; Milo, R., SARS-CoV-2 (COVID-19) by the numbers. *Elife* **2020,** *9*, e57309.

38.   Wang, Y.; Zhang, L.; Sang, L.; Ye, F.; Ruan, S.; Zhong, B.; Song, T.; Alshukairi, A. N.; Chen, R.; Zhang, Z.; Gan, M.; Zhu, A.; Huang, Y.; Luo, L.; Mok, C. K. P.; Al Gethamy, M. M.; Tan, H.; Li, Z.; Huang, X.; Li, F.; Sun, J.; Zhang, Y.; Wen, L.; Li, Y.; Chen, Z.; Zhuang, Z.; Zhuo, J.; Chen, C.; Kuang, L.; Wang, J.; Lv, H.; Jiang, Y.; Li, M.; Lin, Y.; Deng, Y.; Tang, L.; Liang, J.; Huang, J.; Perlman, S.; Zhong, N.; Zhao, J.; Malik Peiris, J. S.; Li, Y.; Zhao, J., Kinetics of viral load and antibody response in relation to COVID-19 severity. *The Journal of Clinical Investigation* **2020**.

39.   Pan, Y.; Zhang, D.; Yang, P.; Poon, L. L. M.; Wang, Q., Viral load of SARS-CoV-2 in clinical samples. *The Lancet Infectious Diseases* **2020,** *20* (4), 411-412.

40.   Weissleder, R.; Lee, H.; Ko, J.; Pittet, M. J., COVID-19 diagnostics in context. *Science Translational Medicine* **2020,** *12* (546), eabc1931.

41.   Russo, L.; Sanchez-Purra, M.; Rodríguez-Quijada, C.; Leonardo, B. M.; Puntes, V.; Hamad-Schifferli, K., Detection of resistance protein A (MxA) in paper-based immunoassays with surface enhanced Raman spectroscopy with AuAg nanoshells. *Nanoscale* **2019,** *11* (22), 10819-10827

42.   Sánchez-Purrà, M.; Carré Camps, M.; de Puig Guixé, H.; Bosch, I.; Gehrke, L.; Hamad-Schifferli, K., SERS-based sandwich immunoassays for multiplexed detection of Zika and dengue viral biomarkers. *ACS Infectious Diseases* **2017,** *3* (10), 767–776.

43.   Babak Y. Moghadam, K. T. C., and Jonathan D. Posner, Two Orders of Magnitude Improvement in Detection Limit of Lateral Flow Assays Using Isotachophoresis. *Analytical Chemistry* **2015,** *87*, 1009-1017.

44.   Qin, Z.; Chan, W. C. W.; Boulware, D. R.; Akkin, T.; Butler, E. K.; Bischof, J. C., Significantly Improved Analytical Sensitivity of Lateral Flow Immunoassays by Using Thermal Contrast. *Angewandte Chemie International Edition* **2012,** *51* (18), 4358-4361.

45.   Vashist, S. K.; Luppa, P. B.; Yeo, L. Y.; Ozcan, A.; Luong, J. H. T., Emerging Technologies for Next-Generation Point-of-Care Testing. *Trends in Biotechnology* **2015,** *33* (11), 692-705.

SYNOPSIS TOC